Enhancement of the crystalline electric field by the conduction electrons in $Tm_xLa_{1-x}Te$

T. Matsumura* and K. A. McEwen
Department of Physics and Astronomy, University College London, Gower Street, London WC1E 6BT, United Kingdom

R. S. Eccleston
ISIS Facility, CLRC Rutherford Appleton Laboratory, Chilton, Didcot OX11 0QX, United Kingdom

T. Suzuki
Department of Physics, Graduate School of Science, Tohoku University, Sendai, 980-8578, Japan
(Received 14 May 2002; published 13 September 2002)

The physical properties of $Tm_xLa_{1-x}Te$ for $x=0.05$ and 0.5 have been investigated by electrical resistivity, magnetic susceptibility, magnetization, and specific heat measurements and by inelastic neutron scattering. It is shown that the Tm ion experiences a large crystalline electric field (CEF) in a metallic environment at a low concentration of $x=0.05$. The level scheme for $x=0.05$ is determined to be $\Gamma_7-\Gamma_8(10\ \mathrm{meV})-\Gamma_6(17.6\ \mathrm{meV})$ by neutron scattering, which is consistent with the bulk properties. However, this scheme is completely opposite to the one predicted from the point charge model. Furthermore, since the Tm ions in an insulating system of $Tm_xYb_{1-x}Te$ do not show such a big CEF, the present result indicates that the conduction electrons play an important role in determining the strength of the CEF. The $\Gamma_7\rightarrow\Gamma_8$ excitation is split into some peaks. This is associated with the local structure around the Tm ions: when the number of other Tm ions in the first-nearest-neighbor rare-earth sites increases, the excitation energy decreases. At $x=0.5$, the CEF excitation disappears and only a broad quasielastic scattering is observed. The excitation spectrum is only reproduced by two Gaussian spectral functions both centered at zero energy.

DOI: 10.1103/PhysRevB.66.104410 PACS number(s): 75.20.Hr, 75.30.Mb, 75.40.Cx, 75.40.Gb

I. INTRODUCTION

Among the rare-earth compounds that exhibit anomalous physical properties originating from the instability of the $4f$ electrons, the Tm monochalcogenides have attracted particular interest in that two magnetic states are involved in the process of valence fluctuation between Tm^{2+} $(4f^{13}, J=7/2)$ and Tm^{3+} $(4f^{12}, J=6)$.[1] This peculiarity, in contrast to Ce- or Yb-based compounds where one valence state is nonmagnetic, has been considered to be the origin of the mysterious magnetic and transport properties of these systems.[2,3] TmSe is of special interest as the only mixed-valent compound ever found that exhibits magnetic order. The two valence states have actually been observed in the antiferromagnetic phase by resonant magnetic x-ray scattering.[4] Apart from the magnetic order, TmSe and the diluted systems of $Tm_xY_{1-x}Se$ and $Tm_xLa_{1-x}Se$ also display anomalous behavior such as the $\ln T$ dependence of the resistivity, which has been discussed in terms of the Kondo effect.[5,6] The temperature dependence of the quasielastic linewidth and the inelastic magnetic scattering at 10 meV observed in neutron scattering studies are also important characteristics of the mixed valent ground state in TmSe and $Tm_xY_{1-x}Se$.[7–9] TmS and the diluted system of $Tm_xY_{1-x}S$ also exhibit similar anomalies.[10,11] However, there has been no consistent explanation for these phenomena. Crystalline electric field (CEF) splittings also have not been observed for these valence fluctuating compounds.

Although TmTe has a relatively stable valence, it seems to be close to valence fluctuation. One reason is that it exhibits an insulator-to-metal transition at 2 GPa where the valence fluctuation also occurs and similar electric properties to TmSe are observed.[12–15] Another reason is that a CEF splitting of the $J=7/2$ ground state is not observed clearly.[16] In order to understand the wide variety of behavior of the $4f$ electrons in the Tm monochalcogenides, it is worth studying a system that is expected to have a more stable valence state. The purpose of the present study is to investigate the local properties of isolated Tm ions in $Tm_xLa_{1-x}Te$, which have not previously been studied, using a sample with $x=0.05$. We also describe the results on a much more concentrated sample with $x=0.5$, in which the interaction between Tm ions becomes dominant.

TmTe is a magnetic semiconductor with Tm^{2+} and Te^{2-}, while LaTe is a monovalent metal with La^{3+} and Te^{2-}. Therefore, if the valence of Tm is $2+$ throughout the concentration, the substitution of La for Tm means the introduction of one conduction electron per formula unit. One of the reasons we chose La, not Lu, as a substitute is that the volume change due to the substitution is much smaller for La than for Lu: the volume of LaTe ($a=6.421$ Å) is 103% of that of TmTe ($a=6.354$ Å), while the volume of LuTe ($a=5.961$ Å) is only 82.6% of that of TmTe.[17]

Our experiment had a number of principal aims. First, which valence state a Tm ion takes in the conduction electron sea of LaTe, i.e., divalent, trivalent, or mixed valent, is not yet an established fact. Second, whether $Tm_xLa_{1-x}Te$ shows a Kondo-like $\ln T$ anomaly in resistivity is a valuable piece of information because $Tm_xY_{1-x}Se$, $Tm_xLa_{1-x}Se$, and $Tm_xY_{1-x}S$ systems all exhibit the $\ln T$ anomaly. Third, whether or not CEF excitations are observed is also an important characteristic to evaluate the stability of the $4f$ electrons.

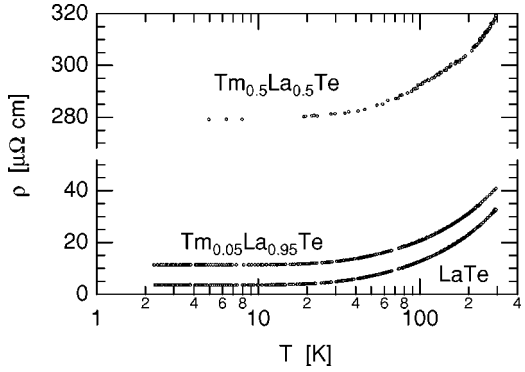

FIG. 1. Temperature dependence of the electrical resistivity of $Tm_xLa_{1-x}Te$. Note the break in the vertical scale.

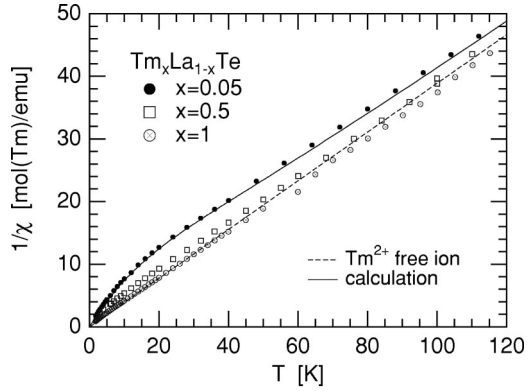

FIG. 2. Temperature dependence of the inverse magnetic susceptibility of $Tm_xLa_{1-x}Te$.

II. RESULTS AND ANALYSIS

The samples were prepared by the Bridgeman method in sealed tungsten crucibles using a high-frequency induction furnace. High-purity thulium and lanthanum metals (Ames Laboratory) and 99.9999% tellurium (High Purity Chemicals Co Ltd., Japan) in a stoichiometric ratio were directly sealed into a tungsten crucible in vacuum by electron beam welding. No prereaction in quartz tubes was performed to avoid possible contamination by quartz. Single crystals were grown by moving down the crucible out of the high-frequency coil at a speed of about 2 mm/h from a temperature about 1900 °C.

A. Electrical resistivity

The electrical resistivity was measured by a conventional four-probe method using rectangular samples with lengths of 3–4 mm and widths and thicknesses of about 0.7 mm. Figure 1 shows the temperature dependence of the electrical resistivity. The three curves for $x=0$, 0.05, and 0.5 are almost parallel with each other. There is no particular anomaly, at least down to 2 K, such as a Kondo-type $\ln T$ dependence as is observed in $Tm_xY_{1-x}Se$, $Tm_xLa_{1-x}Se$, and $Tm_xY_{1-x}S$. This result suggests that the Tm ions in $Tm_xLa_{1-x}Te$ have stable valence states and have little mixing with the conduction electrons. This is consistent with other experimental results described in the following sections.

B. Magnetic susceptibility

The magnetic susceptibility of the samples was measured with a superconducting quantum interference device(SQUID) magnetometer (Quantum Design) from 1.8 K to 300 K. LaTe was also measured but it showed only Pauli paramagnetism with $\chi=2.66\times10^{-5}$ [emu/mol], which was almost temperature independent and negligibly small compared with the susceptibility of $Tm_{0.05}La_{0.95}Te$. Figure 2 shows the temperature dependence of the inverse magnetic susceptibility. This result clearly demonstrates that the Tm ions are divalent throughout the concentration range. Furthermore, the data for $x=0.05$ exhibits an anomaly due to CEF.

Since the crystal structure is NaCl type, the Hund's rule ground multiplet of Tm^{2+} $(4f^{13}, J=7/2)$ splits into Γ_8 quartet, Γ_7 doublet, and Γ_6 doublet states under a cubic CEF. In a previous report we analyzed this $1/\chi$ data by a CEF model of $\Gamma_7-\Gamma_8(12.1\ \text{meV})-\Gamma_6(21.2\ \text{meV})$, which corresponds to $x=-0.95$ and $W=-0.67$ meV in the Lea-Leask-Wolf(LLW) parameters.[18] This level scheme explains the bulk properties of magnetic susceptibility, magnetization, and specific heat in magnetic fields quite nicely. However, as will be described in the next subsection, the correct level scheme has been determined by the neutron scattering experiment. The solid line in the figure is the calculated susceptibility for this newly determined level scheme, $\Gamma_7-\Gamma_8(10\ \text{meV})-\Gamma_6(17.6\ \text{meV})$, which satisfactorily explains the $1/\chi$ data.

In $Tm_{0.5}La_{0.5}Te$ the corresponding anomaly becomes much weaker. It should be noted that we cannot ascribe this slight anomaly to CEF since the inelastic neutron spectrum for $x=0.5$ is completely different from that for $x=0.05$ and there are no clear peaks from CEF levels.

C. Inelastic neutron scattering

Inelastic neutron scattering experiments have been performed using the HET spectrometer at the ISIS pulsed neutron source. HET is a chopper spectrometer in which a single incident neutron energy is selected and the final energy and momentum transfer are analyzed by the time of flight and the detector angle. The first detector bank covers low scattering angles from $\phi=3°$ to 7° at a distance of 4 m from the sample, and the second one covers from $\phi=9°$ to $\phi=29°$ at a distance of 2.5 m. There are two more detector banks covering high scattering angles from $\phi=110°$ to $\phi=140°$ which we use to estimate the contribution from phonon scattering and to check the scattering-vector dependence of magnetic scattering. The scattering intensity was put on an absolute scale in [mb/meV/sr/f.u.] by comparing the intensity with that of the incoherent scattering from a vanadium standard sample measured under the same incident beam conditions.

A collection of small pieces of crystals with total mass 18.6 g was wrapped in aluminum foil and attached to a closed-cycle refrigerator. A Fermi chopper that gives a high

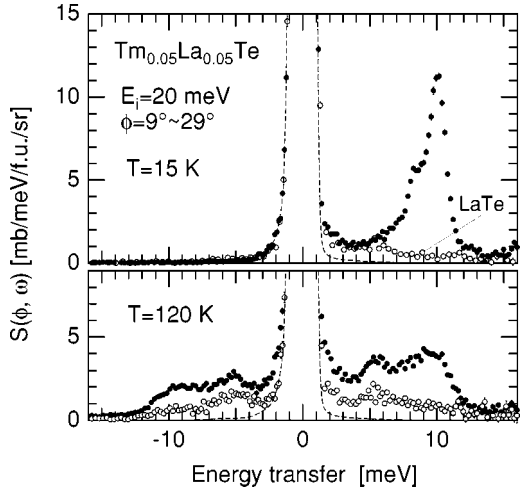

FIG. 3. Neutron scattering function $S(\phi,\omega)$ per formula unit of $Tm_{0.05}La_{0.95}Te$ averaged over the detectors with scattering angles from 9° to 29° on the 2.5 m bank. $S(\phi,\omega)$ of LaTe as a phonon reference material measured under the same conditions is also shown. The dotted line is the measured spectrum of a vanadium standard sample normalized to the same intensity, representing the resolution function at $\hbar\omega=0$.

incident neutron flux, with a corresponding relaxed resolution, was used to improve the statistics of the small magnetic signals from the $Tm_{0.05}La_{0.95}Te$ sample, which included only 587 mg of Tm. LaTe was measured as the phonon reference material.

1. $Tm_{0.05}La_{0.95}Te$

Figure 3 shows the neutron scattering function $S(\phi,\omega)$ for $Tm_{0.05}La_{0.95}Te$ and LaTe measured at an incident energy of 20 meV. Before this measurement, we checked that there was no other magnetic excitation at least up to 50 meV. Since the scattering intensities measured by the detectors with scattering angles from 9° to 29° only showed a weak decrease with increasing angle, following the magnetic form factor of Tm^{2+}, the whole spectra were averaged from 9° to 29° as shown in the figure. For the inelastic scattering at 10 meV, the scattering vector and the magnetic form factor at $\phi=9°$ are 1.1 $Å^{-1}$ and 0.98, respectively, and at $\phi=29°$ they are 1.5 $Å^{-1}$ and 0.94, respectively. The full width at half maximum (FWHM) due to the instrumental resolution decreases from 1.3 meV at $\hbar\omega=0$ meV to about 0.6 meV at $\hbar\omega=10$ meV.

The magnetic part of the scattering function after subtraction of the spectrum of LaTe, taking into account the difference of nuclear scattering length between La and Tm, is shown in Fig. 4. Although correct estimation around $\hbar\omega=0$ was not possible due to the magnetic intensity being much weaker than the large incoherent scattering intensity, the signal from the quasielastic scattering at 120 K may be successfully extracted.

It can be seen that, at 15 K, two peaks are clearly resolved at 10 meV and 8.4 meV. As we already know that Tm ions are 2+, allowing Γ_8, Γ_7, and Γ_6 CEF levels under cubic symmetry, and since there is no dipolar transition probability

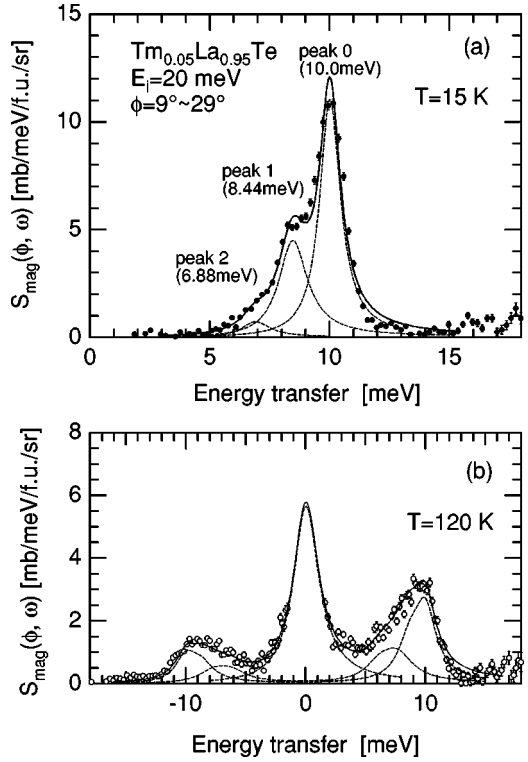

FIG. 4. Magnetic part of the scattering function of $Tm_{0.05}La_{0.95}Te$ per formula unit. Solid lines are the fits with Lorentzian spectral functions. Dashed lines represent contributions from each peak.

between Γ_6 and Γ_7, one might be inclined to conclude that the ground state is the Γ_8 quartet and the two doublets are located at the corresponding peak positions. Indeed, the integrated intensities of the two peaks at 15 K are well reproduced by the calculation which assumes the level scheme of $\Gamma_8-\Gamma_7(8.4\text{ meV})-\Gamma_6(10\text{ meV})$; the integrated intensities as deduced from a fit with two Lorentzian spectral functions are 250 [mb/sr/Tm] for the peak at 8.4 meV and 378 [mb/sr/Tm] for the peak at 10 meV, respectively, while the calculated values are 262 [mb/sr/Tm] and 339 [mb/sr/Tm], respectively.

Although the Γ_8 ground-state model can explain the neutron scattering results if we assume cubic symmetry, it seriously contradicts the bulk properties. It is impossible to reproduce the magnetization and specific heat in magnetic fields. The bulk properties support the Γ_7 ground state.

Special care should be paid to the local symmetry of a Tm ion since the cubic symmetry is broken in a diluted system. This leads to a splitting of the Γ_8 quartet into two Kramers doublets. This effect could be manifested in experiments as a broadening, shift or splitting of an inelastic line as has been studied in detail in the $R_x(Sc,Y,La)_{1-x}Al_2$ system.[19]

We have analyzed the spectra in Fig. 4 assuming the ground state to be a Γ_7 doublet. We also consider that the excitation energy of the $\Gamma_7\rightarrow\Gamma_8$ transition differs from one ion to another depending on its local environment. Since the concentration of Tm is 5%, there is a possibility that some of the 12 first nearest-neighbor (1st NN) rare-earth sites are occupied by other Tm ions. When all of them are occupied

TABLE I. (a) Number of Tm ions N_{Tm} in the 1st nearest neighbor rare-earth sites and its probability for $Tm_{0.05}La_{0.95}Te$ assuming a random distribution of Tm. (b) Peak number indicated in Fig. 4 and the ratio of the integrated intensity as deduced from a fit with Lorentzian spectral functions.

(a) Calculation		(b) Experiment	
N_{Tm}(1st NN)	Probability	Peak No.	Intensity ratio
0	54%	0	61±2.4 %
1	34%	1	34±2.6 %
2	9.9%	2	5.4±1.3 %
3	1.7%	3	–

by La, the local symmetry would be close to cubic; otherwise, the symmetry would be more broken. The number of other Tm ions in the 1st NN sites and its probability when the Tm ions are distributed randomly are listed in Table I.

The magnetic contribution of the inelastic scattering at 15 K in Fig. 4(a) has been fitted with three Lorentzian spectral functions where the peak intensities, positions, and widths are treated as free parameters. The ratios of the integrated intensities obtained for the three peaks are listed in Table I. We notice that they are in very good agreement with the calculated probabilities of the number of Tm ions in the 1st NN sites. It should be noted that the intensity of peak 0 is slightly overestimated because the tail of the peak around 12 meV is not fitted very well owing to the characteristic shape of the resolution function, which is not taken into account in the fit. We can then ascribe the peak 0 at 10 meV to the $\Gamma_7 \rightarrow \Gamma_8$ excitation when all of the 12 1st NN rare-earth sites are occupied by La; the peak 1 at 8.44 meV to the same excitation when one of the 1st NN sites is occupied by Tm, and the peak 2 at 6.88 meV corresponds to the excitation when two of the 1st NN sites are occupied by other Tm. It is worth noting that the interval between the peaks is 1.56 meV.

The spectrum of the magnetic scattering at 120 K shown in Fig. 4(b) has been fitted with five Lorentzian spectral functions; one is the elastic peak at $\hbar\omega=0$, two correspond to the $\Gamma_7 \rightarrow \Gamma_8$ excitation composed of peak 0 and 1, and the other two correspond to the $\Gamma_8 \rightarrow \Gamma_6$ excitation also composed of peak 0 and 1. We have neglected the contribution of peak 2. The same intensity ratio of peak 0 to 1 with that at 15 K has also been assumed. Since the $\Gamma_8 \rightarrow \Gamma_6$ excitation for peak 0 can be recognized at 7.6 meV, we conclude that the CEF level scheme of $Tm_{0.05}La_{0.95}Te$ is $\Gamma_7(0\ \text{meV}) - \Gamma_8(10\ \text{meV}) - \Gamma_6(17.6\ \text{meV})$ when there is no other Tm ion in the 1st NN rare-earth sites and the local symmetry is close to cubic.

Table II shows the parameters of the fit. The calculated integrated intensities for the obtained CEF level scheme, which is further weighted according to the ratio in Table I to estimate the value for peak 0, are also shown so as to be compared. On increasing the temperature from 15 K to 120 K, we first notice that the widths of the peaks become broader. Taking into account the width of the resolution, the intrinsic width of the $\Gamma_7 \rightarrow \Gamma_8$ excitation for peak 0 is estimated to be about 0.74 meV at 15 K and 1.9 meV at 120 K, respectively, and the intrinsic width of the elastic peak at 120 K is again estimated to be about 1.9 meV at 120 K. Second, the intensity seems to shift from the inelastic peaks to the elastic peak, although it is difficult to describe detailed behavior because two of the intensities at 15 K have not been obtained. We note that the static susceptibility obtained from the integration of the spectrum at 120 K is 0.022 [emu/mol], in good agreement with 0.0203 [emu/mol] from the bulk susceptibility measurement; this indicates that the absolute values are reasonable.

TABLE II. Peak position $\hbar\omega$, integrated intensity I, and FWHM of the Lorentzian spectral functions obtained from the fit of the magnetic scattering function of $Tm_{0.05}La_{0.95}Te$. The parameters for the inelastic peaks are shown only for peak 0. I_{calc} is the intensity calculated from the CEF level scheme.

Temperature [K]	15 K	120 K
Elastic peak		
$\hbar\omega$ [meV]	0	0
I [mb/Tm/sr]	-	458±22
I_{calc} [mb/Tm/sr]	391	345
FWHM [meV]	-	2.6±0.33
$\Gamma_7 \rightarrow \Gamma_8$ (peak 0)		
$\hbar\omega$ [meV]	10.01±0.008	9.99±0.094
I [mb/Tm/sr]	366±8.6	90±20
I_{calc} [mb/Tm/sr]	318	100
FWHM [meV]	1.06±0.022	2.14±0.15
$\Gamma_8 \rightarrow \Gamma_6$ (peak 0)		
$\hbar\omega$ [meV]	-	7.6±0.45
I [mb/Tm/sr]	-	42±17
I_{calc} [mb/Tm/sr]	0.18	38
FWHM [meV]	-	3.1±0.42

2. $Tm_{0.5}La_{0.5}Te$

When the concentration of Tm is increased to 50%, the inelastic peaks of the CEF excitation disappear and a broad quasielastic scattering peak appears. Since the magnetic contribution to the total scattering becomes much larger at 50%, it was also possible to separate the elastic component of the magnetic scattering from the incoherent scattering at $\hbar\omega=0$.

Figure 5 shows the magnetic part of the scattering function obtained by subtracting contributions of phonon and incoherent scattering. This treatment can be justified by the result that the integrated intensity agrees with the measured bulk susceptibility as shown in the inset figure. The scattering function consists of a sharp elastic component and a broad inelastic component. Concerning the inelastic part, after trying several fitting functions, we have found that it can be reproduced by two Gaussian spectral functions both centered at $\hbar\omega=0$. Lorentzian spectral functions give a longer tail up to higher energies, leading to poorer fits. Fitting functions with one or two finite energy excitations due to CEF levels also cannot give better fits. The parameters obtained are listed in Table III. At high temperatures, the quasielastic

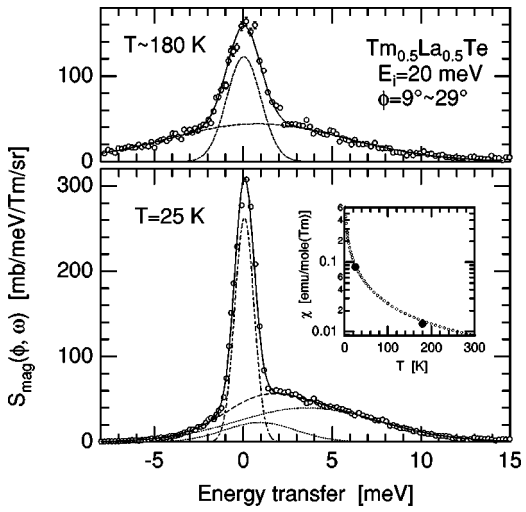

FIG. 5. Magnetic part of the scattering function of $Tm_{0.5}La_{0.5}Te$ per Tm ion. Solid lines are the fits with Gaussian spectral functions. Each component is indicated by the dashed lines. The broad quasielastic scattering at 25 K consists of two Gaussians indicated by the two dotted lines. The inset figure compares the static susceptibility obtained from the integration of the spectra with the measured bulk magnetic susceptibilities indicated by smaller points.

peak can be reproduced by a single Gaussian as shown by the result at 180 K.

The sharp elastic peak at 25 K can be fit by a Gaussian with its width almost equal to the instrumental resolution, indicating that this peak is resolution limited. At high temperatures the width of the elastic peak becomes broader than the resolution as seen in the spectrum at 180 K. It is difficult to determine from the present experiment whether this is expressed by a Gaussian or a Lorentzian spectral function. Both can fit the data by changing the weight of the other broad Gaussian quasielastic peak. Apart from this ambiguity, we can at least conclude that the width of this peak is as large as that of the quasielastic peak of $Tm_{0.05}La_{0.95}Te$ at 120 K. This indicates that they are of the same origin.

TABLE III. Energy position $\hbar\omega$, intensity I, and FWHM of the Gaussian spectral functions obtained from the fit of the magnetic scattering function of $Tm_{0.5}La_{0.5}Te$. FWHM for 25 K is a resolution limited width.

Temperature [K]	25 K	180 K
Elastic peak		
$\hbar\omega$ [meV]	0	0
I [mb/Tm/sr]	353±2	267±4
FWHM [meV]	1.273±0.006 (reso.)	2.18±0.03
First quasielastic peak		
$\hbar\omega$ [meV]	0	0
I [mb/Tm/sr]	303±3	482±4.2
FWHM [meV]	10.83±0.05	11.33±0.08
Second quasielastic peak		
$\hbar\omega$ [meV]	0	-
I [mb/Tm/sr]	106±3	-
FWHM [meV]	4.9±0.1	-

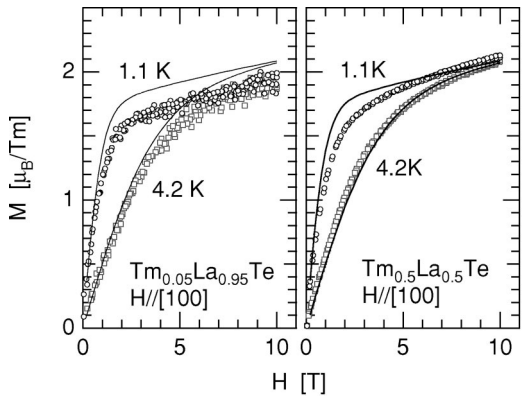

FIG. 6. Magnetization of $Tm_{0.05}La_{0.95}Te$ and $Tm_{0.5}La_{0.5}Te$ along the [100] direction at 1.1 K and 4.2 K. The solid lines are the calculated magnetization curves for respective temperatures considering only the CEF effect: $\Gamma_7-\Gamma_8(10\ \text{meV})-\Gamma_6(17.6\ \text{meV})$.

D. Magnetization and specific heat

It is valuable to study the magnetization and specific heat of these compounds with the microscopic knowledge obtained in the neutron scattering experiment. The magnetization was measured by the extraction method and the specific heat was measured by a conventional quasiadiabatic heat pulse method, both for the magnetic fields along the fourfold [100] axis. The magnetic specific heat was obtained by subtracting the phonon contribution; for $Tm_{0.05}La_{0.95}Te$ the specific heat of LaTe was subtracted and for $Tm_{0.5}La_{0.5}Te$ the averaged specific heat of LaTe and YbTe was subtracted.

In Fig. 6 the magnetization of $Tm_{0.05}La_{0.95}Te$ at 4.2 K and 1.1 K for the field along the [100] axis is shown. Rather scattered data points are due to small signals from only 5% concentration of Tm. The solid lines are the calculated magnetization curves for the model with the CEF and the Zeeman Hamiltonians only. The level scheme that has been determined in Sec. II C 1 has been used. The overall behavior is well reproduced by the calculation. This CEF level scheme can also explain the specific heat results. Figure 7 shows the magnetic specific heat of $Tm_{0.05}La_{0.95}Te$ in magnetic fields. At zero field no magnetic specific heat appears at least down to 1.5 K. Application of a magnetic field induces a Schottky anomaly due to the Zeeman splitting of the Γ_7 ground state. Overall features, especially the peak positions, are well reproduced by the calculation. To summarize, the three bulk properties $\chi(T)$, $M(H)$, and $C_{\text{mag}}(H,T)$ can be explained by the CEF level scheme obtained in Sec. II C 1 very well.

With regard to $Tm_{0.5}La_{0.5}Te$ in which CEF excitations are not observed, although the $M(H)$ curves are very similar to those of $Tm_{0.05}La_{0.95}Te$, the behavior of the magnetic specific heat is completely different as shown in Fig. 8. The magnetic specific heat is observed even at zero field. This is considered to be caused by intersite magnetic correlations, which should be the origin of the broad quasielastic scattering. The low-temperature part of the zero-field specific heat seems to exhibit T-linear behavior with $C=0.31T$ [J/mol

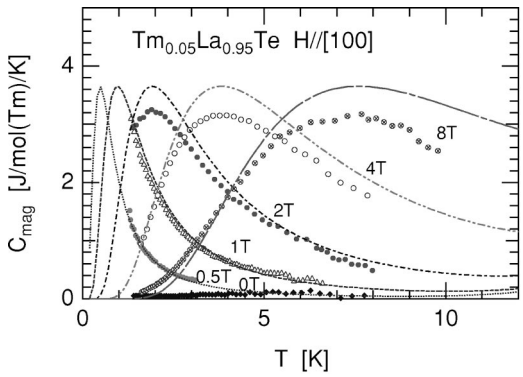

FIG. 7. Magnetic specific heat of $Tm_{0.05}La_{0.95}Te$ in magnetic fields along the [100] axis. The solid lines are the calculated specific heat for respective magnetic fields considering only the CEF effect: $\Gamma_7-\Gamma_8(10\ \mathrm{meV})-\Gamma_6(17.6\ \mathrm{meV})$.

(Tm)/K], which might be related with the spin correlations that give rise to quasielastic scattering. When a magnetic field is applied, an additional contribution to the specific heat due to the Zeeman splitting of the ground state becomes visible as in $Tm_{0.05}La_{0.95}Te$.

III. DISCUSSION

A novel effect in $Tm_{0.05}La_{0.95}Te$ is the appearance of a large CEF splitting. The fact that the insulating TmTe exhibits only a small and ambiguous CEF splitting less than 2 meV is already known.[16,20,21] This situation does not change when diluted with Yb, where the insulating environment is preserved because the Yb ion becomes $2+$.[22] On the other hand, in the present case, when a Tm ion is diluted in a metallic environment of LaTe, it experiences a large CEF. This difference is clearly demonstrated by the magnetic susceptibility shown in Fig. 9. While $Tm_{0.05}La_{0.95}Te$ exhibits a clear CEF anomaly, $Tm_{0.03}Yb_{0.97}Te$ does not show any CEF anomaly.

Although the simplest model of the CEF is the point charge model (PCM), there are few actual examples where the PCM is sufficient. A number of examples have been reported where the PCM cannot explain the observed splitting

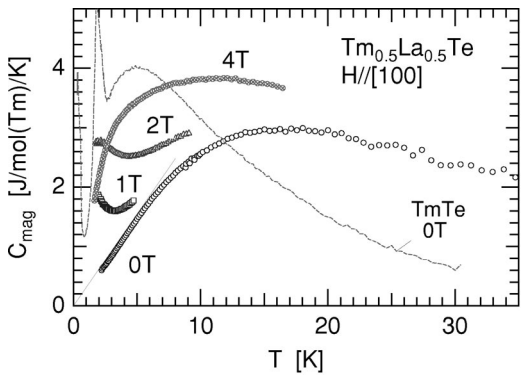

FIG. 8. Magnetic specific heat of $Tm_{0.5}La_{0.5}Te$ under magnetic fields along the [100] axis. The line indicates the T-linear term of $C=0.31T$ [J/mol (Tm)/K]. Magnetic specific heat of TmTe is shown for reference.

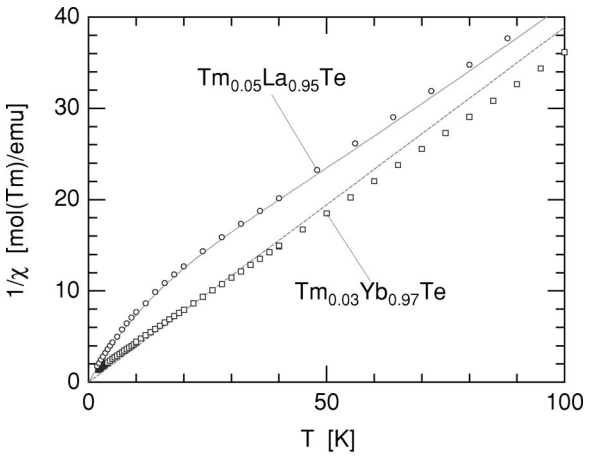

FIG. 9. Inverse magnetic susceptibility of $Tm_{0.05}La_{0.95}Te$ and $Tm_{0.03}Yb_{0.97}Te$; the former corresponds to a Tm ion in the metallic environment and the latter to the insulating environment.

and the contribution of the conduction electrons is much more important.[19,23–26] Rare-earth monopnictides and chalcogenides have been considered as an example to which the PCM can be applied, though we need to use effective charges.[27] However, strangely, all the measured CEF parameters of $A_4\langle r^4\rangle$ and $A_6\langle r^6\rangle$ for Ce, Pr, and Nd pnictides and chalcogenides can be reproduced by the nearest-neighbor PCM assuming an effective charge of -2,[28–33] in spite of the fact that the anion valences, band structures, and the number of carriers are quite different between pnictides and chalcogenides. Furthermore, the high-pressure experiments for rare-earth monopnictides show opposite behavior to what is expected from the PCM.[34,35]

In $Tm_{0.05}La_{0.95}Te$, the CEF parameters are contradictory to the PCM. The level scheme of $\Gamma_7-\Gamma_8(10\ \mathrm{meV})-\Gamma_6(17.6\ \mathrm{meV})$ corresponds to the LLW parameters of $x=-0.947$ and $W=-0.573$ meV, i.e., $A_4\langle r^4\rangle=-5.223$ meV and $A_6\langle r^6\rangle=-0.163$ meV. This is completely different from what is expected from the PCM. Although the value of x being close to -1 is consistent with the PCM, the sign of W is opposite. In view of the fact that $Tm_{0.03}Yb_{0.97}Te$ does not show a CEF splitting and that the difference of La^{3+} and Yb^{2+} does not give such big change in CEF (within the PCM calculation), it is apparent that the CEF is determined by some interaction of $4f$ electrons with conduction electrons, although the mechanism is unclear. Many factors must be involved to the CEF. Point charges, indeed, may be the primitive source of the field. However, what is more important should be how it is mediated by the conduction and valence electrons to the $4f$ electrons, which is different from one compound to another.

In recent calculations, Brooks *et al.* have viewed crystal field excitations as quasiparticles composed of an *f*-electron excitation plus an associated cloud of shielding conduction electrons.[36] It is to be expected that the shielding cloud, which is the reaction of the solid to the original bare *f* excitation, will depend on the local Tm^{2+} and La^{3+} environment and, hence, that the crystal field excitation energy will vary accordingly. From our analysis of the peak structure in Fig. 4(a), we have proposed a model where the energy level of

the Γ_8 state decreases by 1.56 meV when the number of Tm^{2+} ions in the 1st NN rare-earth sites increases by 1. On the other hand, we do not have clear evidence to exclude the possibility that the multipeak structure is given by the Γ_8 quartet being split into two doublets, which of course differs from site to site. However, if the substitution of Tm^{2+} only results in a splitting of the Γ_8 state, we cannot explain the fact that the CEF excitations disappear in $Tm_{0.5}La_{0.5}Te$ and $Tm_{0.03}Yb_{0.97}Te$. The effect of lowered symmetry may probably be reflected in the width of each peak in Fig. 4(a). The multipeak structure with an interval of 1.56 meV is supposed to be caused by 2+ ions in the 1st NN rare-earth sites, each of which captures one conduction electron, resulting in reduction of the local density of conduction electrons.

The disappearance of a clear CEF excitation in $Tm_{0.5}La_{0.5}Te$ may probably be related to the reduction of the number of conduction electrons. If a disturbance of the CEF by a random distribution of different valences of Tm^{2+} and La^{3+} were the case, some broad excitation should be observed, which is not the case. Only quasielastic scatterings are observed. The two Gaussian components at 25 K can be ascribed to two correlation times, the fast one and the slow one. Though it is speculated that this spin correlation is associated with the behavior of the low-temperature magnetic specific heat, the detailed mechanism is an open question.

Finally, concerning the broadening of the peaks, a number of possibilities can be considered: the broadening due to nonstoichiometry, disturbed surroundings, interaction with phonons, and interaction with conduction electrons. Among these possibilities, the temperature dependence of the intensities and the widths of the observed peaks in the present system seems to reflect the coupling with the conduction electrons, which is modeled by a theory by Becker, Fulde, and Keller (BFK).[37] According to the theory, when a coupling between the local moment and the conduction electrons are introduced, on increasing temperature, the widths of the elastic and the inelastic peak increase, the inelastic peak moves to lower energies, and the intensity of the inelastic peak is transferred to that of the elastic peak. Although quantitative analysis has not been performed in the present study, the obtained widths of the elastic peak at high temperature that are listed in Table II and III are typical values for stable $4f$ moments. The result that the intensity of the inelastic peak transfers to that of the quasielastic peak with increasing the temperature is also consistent with the BFK theory.

IV. CONCLUSIONS

We have measured the bulk properties and the neutron scattering functions of $Tm_xLa_{1-x}Te$ for $x=0.05$ and 0.5. The sample for $x=0.05$ has a physical meaning that a single Tm ion is located in the conduction electron sea of LaTe, which should be compared with the insulating environment in $Tm_xYb_{1-x}Te$. Tm ions have been found to exist as stable 2+ ions all through the concentration range. Furthermore, it has been found that the metallic environment of LaTe produces a large CEF. The neutron scattering measurements established the level scheme of $\Gamma_7-\Gamma_8(10\ \mathrm{meV})-\Gamma_6(17.6\ \mathrm{meV})$, which is also consistent with the bulk properties of $\chi(T)$, $M(H)$, and $C_{\mathrm{mag}}(H,T)$. However, this sequence is completely opposite to the one predicted from the point charge model. This is quite unusual when compared with other rare-earth monochalcogenides and monopnictides. In view of the fact that $Tm_{0.03}Yb_{0.97}Te$ does not show a CEF splitting, it is strongly suggested that the conduction electrons play an important role.

In $Tm_{0.5}La_{0.5}Te$ the CEF excitations disappear and a broad quasielastic scattering appears. The neutron scattering function consists of two Gaussian quasielastic components and a sharp elastic component at low temperatures, indicating that magnetic correlations are dominant and a CEF excitation does not exist. This is reflected in the characteristic behavior of the magnetic specific heat at zero field.

The temperature dependence of the intensities and the widths of the inelastic and elastic peaks can be explained by the BFK theory qualitatively, which takes into account the coupling of the local moment with the conduction electrons. The widths have been found to be typical of those for stable $4f$ moments.

ACKNOWLEDGMENTS

T.M. thanks the Japanese Society for the Promotion of Science for support. K.A.M. acknowledges financial support from the UK Engineering and Physical Sciences Research Council.

*Present address: Department of Physics, Graduate School of Science, Tohoku University, Sendai, 980-8578, Japan. Electronic address: tmatsu@iiyo.phys.tohoku.ac.jp

[1] P. Wachter, in *Handbook on the Physics and Chemistry of Rare Earths*, edited by K.A. Gschneidner, Jr., L. Eyring, G.H. Lander, and G.R. Choppin (North-Holland, Amsterdam, 1994), Vol. 19, p. 177.

[2] T. Saso, J. Phys. Soc. Jpn. **58**, 4064 (1989).

[3] C.M. Varma, Solid State Commun. **30**, 537 (1979).

[4] D.B. McWhan, E.D. Isaacs, P. Carra, S.M. Shapiro, B.T. Thole, and S. Hoshino, Phys. Rev. B **47**, 8630 (1993).

[5] P. Haen, O. Laborde, F. Lapierre, and J.-M. Mignot, in *Valence Instabilities*, edited by P. Wachter and H. Boppart (North-Holland, Amsterdam, 1982), p. 423.

[6] P. Haen, H. Bioud, F. Lapierre, and F. Holtzberg, J. Magn. Magn. Mater. **63&64**, 603 (1987).

[7] M. Loewenhaupt and E. Holland-Moritz, J. Appl. Phys. **50**, 7456 (1979).

[8] S.M. Shapiro and B.H. Grier, Phys. Rev. B **25**, 1457 (1982).

[9] E. Holland-Moritz, J. Magn. Magn. Mater. **38**, 253 (1983).

[10] P. Haen, H. Bioud, F. Lapierre, and F. Holtzberg, in *Theoretical and Experimental Aspects of Valence Fluctuations*, edited by L. C. Gupta and S.K. Malik (Plenum, New York, 1987), p. 445.

[11] F. Holtzberg, J. Flouquet, P. Haen, F. Lapierre, Y. Lassailly, and C. Vettier, J. Appl. Phys. **57**, 3152 (1985).

[12] T. Matsumura, T. Kosaka, J. Tang, T. Matsumoto, H. Takahashi, N. Môri, and T. Suzuki, Phys. Rev. Lett. **78**, 1138 (1997).

[13] P. Link, I.N. Goncharenko, J.-M. Mignot, T. Matsumura, and T.

Suzuki, Phys. Rev. Lett. **80**, 173 (1998).
[14] M. Ohashi, N. Takeshita, H. Mitamura, T. Matsumura, T. Suzuki, T. Mori, T. Goto, H. Ishimoto, and N. Môri, J. Magn. Magn. Mater. **226-230**, 58 (2001).
[15] J.-M. Mignot, I.N. Goncharenko, P. Link, T. Matsumura, and T. Suzuki, Hyperfine Interact. **128**, 207 (2000).
[16] E. Clementyev, R. Köhler, M. Braden, J.-M. Mignot, C. Vettier, T. Matsumura, and T. Suzuki, Physica B **230-232**, 735 (1997).
[17] E. Bucher, K. Andres, F.J. di Salvo, J.P. Maita, A.C. Gossard, A.S. Cooper, and G.W. Hull, Jr., Phys. Rev. B **11**, 500 (1975).
[18] K.R. Lea, M.J.M. Leask, and W.P. Wolf, J. Phys. Chem. Solids **23**, 1381 (1962).
[19] B. Frick and M. Loewenhaupt, Z. Phys. B: Condens. Matter **63**, 231 (1986).
[20] T. Matsumura, H. Shida, and T. Suzuki, Physica B **230-232**, 738 (1997).
[21] T. Matsumura, S. Nakamura, T. Goto, H. Amitsuka, K. Matsuhira, T. Sakakibara, and T. Suzuki, J. Phys. Soc. Jpn. **67**, 612 (1998).
[22] E. Clementyev (private communication).
[23] B. Frick and M. Loewenhaupt, Z. Phys. B: Condens. Matter **63**, 213 (1986).
[24] G. Knopp, K. Knorr, H. Wehr, and A.P. Murani, J. Magn. Magn. Mater. **52**, 326 (1985).
[25] D. Schmitt, J. Phys. F: Met. Phys. **9**, 1745 (1979).
[26] D. Schmitt, J. Phys. F: Met. Phys. **9**, 1759 (1979).
[27] R.J. Birgeneau, E. Bucher, J.P. Maita, L. Passel, and K.C. Turberfield, Phys. Rev. B **8**, 5345 (1973).
[28] A. Furrer and U. Tellenbach, Phys. Status Solidi B **71**, K31 (1975).
[29] A. Furrer and E. Warming, J. Phys. C **7**, 3365 (1974).
[30] A. Furrer, J. Kjems, and O. Vogt, J. Phys. C **5**, 2246 (1972).
[31] K.C. Turberfield, L. Passell, R.J. Birgeneau, and E. Bucher, J. Appl. Phys. **42**, 1746 (1971).
[32] A. Dönni, A. Furrer, P. Fischer, and F. Hulliger, Physica B **186-188**, 541 (1993).
[33] J. Rossat-Mignod, J.M. Effantin, P. Burlet, T. Chattopadhyay, L.P. Regnault, H. Bartholin, C. Vettier, O. Vogt, D. Ravot, and J.C. Achart, J. Magn. Magn. Mater. **52**, 111 (1985).
[34] J.E. Schirber, H.T. Weaver, and D.S. Ginley, J. Appl. Phys. **49**, 1469 (1978).
[35] H. Yoshizawa, Y. Okayama, Y. Oohara, H. Takahashi, N. Môri, S. Mitsuda, T. Osakabe, M. Kohgi, Y. Haga, and T. Suzuki, J. Phys. Soc. Jpn. **64**, 617 (1995).
[36] M.S.S. Brooks, O. Eriksson, J.M. Wills, and B. Johansson, Phys. Rev. Lett. **79**, 2546 (1997).
[37] K.W. Becker, P. Fulde, and J. Keller, Z. Phys. B **28**, 9 (1977).